

Atmospheric Outflow of Anthropogenic Semivolatile Organic Compounds from East Asia in Spring 2004

TOBY PRIMBS,[†] STACI SIMONICH,^{*,†,‡} DAVID SCHMEDDING,[‡] GLENN WILSON,[‡] DAN JAFFE,[§] AKINORI TAKAMI,^{||} SHUNGO KATO,[⊥] SHIRO HATAKEYAMA,^{||} AND YOSHIKAZU KAJII[⊥]

Departments of Chemistry and Environmental and Molecular Toxicology, Oregon State University, Corvallis, Oregon 97331, University of Washington—Bothell, Bothell, Washington, Atmospheric Environmental Division, National Institute of Environmental Studies, Tsukuba, Japan, and Applied Chemistry, Faculty of Engineering, Tokyo Metropolitan University, Tokyo, Japan

To estimate the emissions of anthropogenic semivolatile organic compounds (SOCs) from East Asia and to identify unique SOC molecular markers in Asian air masses, high-volume air samples were collected on the island of Okinawa, Japan between 22 March and 2 May 2004. Contributions from different source regions (China, Japan, the Koreas, Russia, and ocean/local) were estimated by use of source region impact factors (SRIFs). Elevated concentrations of hexachlorobenzene (HCB), hexachlorocyclohexanes (HCHs), dichlorodiphenyltrichloroethanes (DDTs), and particulate-phase polycyclic aromatic hydrocarbons (PAHs) were attributed to air masses from China. A large proportion of the variation in the current-use pesticides, gas-phase PAHs, and polychlorinated biphenyl (PCB) concentrations was explained by meteorology. Chlordanes showed a technical mixture profile and similar concentrations regardless of source region. α/γ HCH and *trans/cis* chlordane ratios did not vary significantly with different source regions and had regional averages of 2.5 ± 1.0 and 1.2 ± 0.3 , respectively. Particulate-phase PAH concentrations were significantly correlated (p value < 0.05) with other incomplete combustion byproduct concentrations, including elemental mercury (Hg⁰), CO, NO_x^{*}, black carbon, submicrometer aerosols, and SO₂. By use of measured PAH, CO, and black carbon concentrations and estimated CO and black carbon emission inventories, the emission of six carcinogenic particulate-phase PAHs was estimated to be 1518–4179 metric tons/year for Asia and 778–1728 metric tons/year for China, respectively. These results confirm that East Asian outflow contains significant emissions of carcinogenic particulate-phase PAHs.

* Corresponding author phone: 541-737-9194; fax: 541-737-0497; e-mail: staci.simonich@oregonstate.edu.

[†] Department of Chemistry, Oregon State University.

[‡] Department of Environmental and Molecular Toxicology, Oregon State University.

[§] University of Washington—Bothell.

^{||} National Institute of Environmental Studies.

[⊥] Tokyo Metropolitan University.

Introduction

Atmospheric transport of air pollutants, including anthropogenic semivolatile organic compounds (SOCs) and inorganic trace gases (e.g., CO), from Asian sources to the Pacific coast of North America has been previously identified (1–6). Chemical measurements, coupled with air trajectories, have shown transport across the Pacific can occur in as little as 5–10 days during the winter and spring months (1, 5). Anthropogenic SOC emissions are emitted from a variety of activities including fossil fuel combustion, biomass burning, agriculture, and/or industrial activities. SOC emissions may exist in the gas and/or particle phase in the atmosphere and have a wide range of atmospheric lifetimes (hours to months). Due to their wide range of atmospheric lifetimes, physical–chemical properties, and their emission from a diverse array of anthropogenic sources, SOC emissions may be good molecular markers for differentiating source regions of trans-Pacific air masses as well as different source types.

Research investigating the trans-Pacific atmospheric transport of anthropogenic SOC emissions has primarily focused on the west coast of North America (2, 3, 6). Additional information on the SOC composition of Asian air masses, in the near vicinity of Asia, is needed to assist in the proper identification of trans-Pacific air masses of Asian origin. The primary objectives of this research were to (1) identify the SOC composition of Asian air masses; (2) determine if air masses from different Asian source regions (China, Japan, the Koreas, Russia, and ocean/local) have unique SOC compositions; and (3) to estimate the emission of PAHs from Asia. To our knowledge, this is the first research to characterize the SOC composition of Asian air masses, from distinct source regions, in relation to trans-Pacific atmospheric transport and to estimate the emission of PAHs from Asia and China by use of measured concentrations.

Experimental Procedures

Chemicals. The anthropogenic SOC emissions detected encompass several categories. Polycyclic aromatic hydrocarbons (PAHs) included fluorene (FLO), anthracene (ANT), phenanthrene (PHE), fluoranthene (FLA), pyrene (PYR), retene (RET), benzo[*a*]anthracene (BaA), chrysene/triphenylene (CT), benzo[*b*]fluoranthene (BbF), benzo[*k*]fluoranthene (BkF), benzo[*e*]pyrene (BeP), benzo[*a*]pyrene (BaP), indeno[1,2,3-*cd*]pyrene (IcdP), dibenz[*a,h*]anthracene (DahA), and benzo[*ghi*]perylene (BghiP). Miscellaneous combustion byproducts included 1,3,5-triphenylbenzene (TPB) and levoglucosan (Lev). Polychlorinated biphenyls (PCBs) included PCBs 101, 118, 153, 138, 187, and 183. Pesticides included dichlorodiphenyldichloroethylenes (*o,p'*-DDE and *p,p'*-DDE), dichlorodiphenyltrichloroethane (*o,p'*-DDT), trifluralin (Trif), hexachlorobenzene (HCB), α - and γ -hexachlorocyclohexanes (α -HCH and γ -HCH), metribuzin (Met), heptachlor (Hept), dacthal (Dac), chlorpyrifos (Chlorp), *oxy*-, *trans*-, and *cis*-chlordanes (OC, TC, and CC), *trans*- and *cis*-nonachlors (TN and CN), endosulfans I and II (Endo I and Endo II), endosulfan sulfate (Endo S), and dieldrin (Dield). The atmospheric lifetimes of these SOC emissions range from hours to months. A complete list of the measured SOC emissions, including those not detected in these samples, the isotopically labeled surrogates and internal standards that were used for quantitation, and the origination of all standards and solvents used, has been previously reported (7).

Sampling Site. The sampling site (Hedo Station Observatory, HSO) is located on the northwest coast of the island of Okinawa, Japan [26.8° N, 128.2° E, 60 m above sea level (asl)],

about 200 m from the East China Sea (Figure S11). HSO is an established air monitoring site used to study the outflow of air pollution from Asia (8–10) and is ~800 km from the coast of China. Atmospheric transport times from China, the Koreans, and Japan to the site are ~24–48 h (8). Other simultaneous measurements at HSO during the sampling campaign included submicrometer aerosols (nephelometer), reactive gaseous mercury, particulate-phase mercury, and elemental mercury, which were conducted by the Jaffe Group (University of Washington—Bothell, Seattle, WA) and Frontier Geosciences (Seattle, WA) (10). Other measurements were conducted by the National Institute for Environmental Studies, Tokyo Metropolitan University, and the Acid Deposition and Oxidant Research Center and included meteorological measurements, an Aerodyne Aerosol Mass Spectrometer (AMS), carbon monitor (to measure black carbon and organic carbon), CO, O₃, VOCs, SO₂, NO, and NO_x* (NO_x and some NO_y species).

Sample Collection and Extraction. Eighteen samples (17–24 h in duration) were collected for SOCs from 22 March 2004 to 2 May 2004 by use of a modified high-volume air sampler (Tisch Env. Cleves, OH) (Table S11). The sampler was located on the top of the site building and was calibrated using a standardized orifice manometer kit (Tisch Environmental, Cleves, OH). The sampling flow rate was recorded before and after collection of each sample. Additional information on sample collection and extraction is given in the Supporting Information.

Sample Analysis. Sample analysis was conducted by gas chromatographic mass spectrometry (GC/MS) in selective ion monitoring (SIM) mode with electron capture negative ionization (ECNI) and electron impact (EI) ionization modes (7). Analysis of specific SOCs was divided between the two ionization modes, based on which ionization mode resulted in the lowest instrumental detection limit (7). Instrumental limits of detection ranged from 0.006 to 6.7 pg/μL (7). Limits of quantification, defined as the lowest standard used in the calibration curves, ranged from 0.25 to 50 pg/μL. Estimated method detection limits, calculated by EPA method 8280A, ranged from 0.11 to 114 pg/m³ for GC/MS-EI and from 0.0001 to 6.4 pg/m³ for GC/MS-ECNI (11). Only signals exceeding 3 times the peak-to-peak noise were reported. Details of the ions monitored, instrumental limits of detection, and GC conditions are reported elsewhere (7). 1,3,5-Triphenylbenzene (TCI America) was measured by GC/MS-EI and SIM quantification of ion *m/z* 306 and qualifying ions *m/z* 217, 289, and 228. Levoglucosan (Sigma—Aldrich) was measured by use of quantifying ion *m/z* 204 and qualifying ions *m/z* 217, 333, and 73 by GC/MS-EI after being derivatized.

Quality Assurance Procedures. SOC recoveries ranged from 50% to 118% over the entire analytical method. The bottom polyurethane foam (PUF) plug was used to detect potential SOC breakthrough during sample collection, and the SOC concentration in the bottom PUF plug ranged from 0.06% to 22% of the total gas-phase concentration. Because SOC breakthrough during sampling was not significant, no correction was made. The second quartz fiber filter was used to investigate adsorption of gas-phase SOCs to the filter medium itself. Endo I, Endo II, Trif, and HCB showed occasional adsorption to the quartz fiber filters and no correction was made. Three field blanks were collected during the campaign and consisted of installation of the sampling medium in the high-volume air sampler for 24 h, with the power off. FLO, PHE, FLA, PYR, RET, Trif, Met, HCB, and Chlorp were detected in the field blanks above the quantification limit. The ratio of measured sample concentration to the average field blank concentration ranged (minimum–maximum) as follows: FLO (20–200), PHE (104–942), FLA (72–493), PYR (261–1690), RET (14–175), Trif (6–245), Met (16–51), HCB (261–775), and Chlorp (8–641). Reported SOC

concentrations were field blank and surrogate recovery corrected (SOC concentration were calculated versus the spiked isotopically labeled surrogates).

Trajectories and Data Analysis. Four-day back trajectories were calculated by use of NOAA's ARL HYSPLIT 4.0 model (FNL) (12). For each 24 h sample, seven trajectories were calculated (one every 4 h), which included the start and stop times of the sampling period. At each 4 h interval, three trajectories were calculated (at 60, 250, and 500 m asl) to understand the general air mass flow in the boundary layer where the sampling site is located (elevation 60 m asl). Additionally, the model's precipitation data were included in the data output. S-PLUS version 7.0 (Insightful, Seattle, WA) was used for statistical analysis.

Results and Discussion

Back Trajectories and Source Region Impact Factors. Back trajectories were used to determine the impact of different source regions (China, Korea, Japan, Russia, and ocean/local) on the air masses sampled and was termed source region impact factor (SRIF). The SRIF represents the percentage of time an air mass spent in a given source region in the last 4 days prior to arriving, and being sampled, at HSO. Similar methods, using the amount of time trajectories spent in different regions, have been used by other researchers (6, 13). The higher the SRIF percentage, the more time the sampled air mass spent in a given source region. The SRIF can be used to assess transport time from source regions to HSO by comparing time spent in a given source region to the time spent in other source regions. Additionally, it can be used to determine if the amount of time spent in a given source region impacts the air concentrations of the SOCs at HSO.

Equation 1 shows the details of the calculation of the SRIF. Step 1 was to calculate the 4-day back trajectories for air masses associated with each sample. This was done by calculating seven trajectories for every 24 h sample (one every 4 h for 24 h, including the sample start and stop times). Step 2 was to calculate the time the trajectories spent in a given source region. This was calculated for all source regions [China, Japan, the Koreans, Russia, and ocean/local (which includes the island of Okinawa)]. For each trajectory, the time spent in a given source region (T_{sr}) was identified as a binary response: 1 if it was in the given source region and 0 if it was not. This was repeated each hour for 4 days back in time ($n = 1-96$ h). The final step was to calculate the SRIF by dividing the fraction of the total hours spent in a given source region by 672 h [96 (total no. of hours back) × 7 (no. of trajectories per sample)]. Finally, this was presented as a percentage:

$$\text{SRIF (\%)} = \left\{ \left[\sum_{n=1}^{96} (n(T_{sr} = 1; \text{otherwise} = 0)) \right] \text{ hours} / 672 \text{ hours} \right\} \times 100 \quad (1)$$

SRIFs were calculated for three elevations, 60, 250, and 500 m asl, to assess boundary layer flow. There was no statistically significant difference for the SRIFs between the three elevations (p value < 0.01), and the SRIFs at 250 m asl were used in subsequent calculations to represent atmospheric flow above the ground level of the HYSPLIT model. Table S11 summarizes the site meteorology and the SRIFs for the samples collected at HSO. The 4-day back trajectories associated with the four air samples having the highest SRIFs for China, Japan, Korea, Russia, and ocean/local are shown in Figure 1.

Principal component analysis (PCA) of the SRIFs in Table S11 was used to further classify the samples into source regions. The PCA biplot for the first two principal components

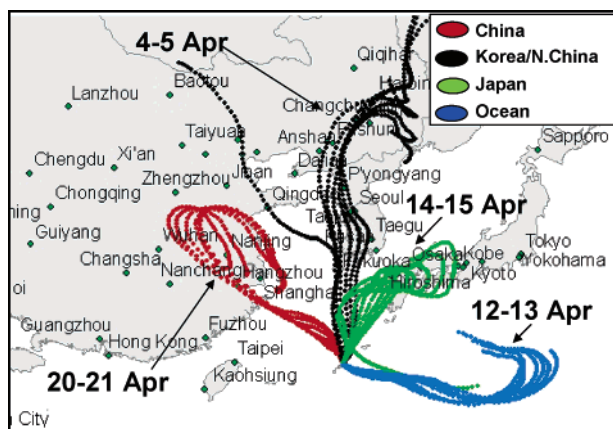


FIGURE 1. Representative 4-day back trajectories (250 m asl) for representative air masses sampled from Japan, China, Pacific Ocean, and Korea during the 6-week campaign. Each dot represents 1 h back in time. Cities with populations greater than 1 million people are labeled.

explained 90.7% of the variation in the original data (Figure SI2). The clustering from this biplot was further used to classify the samples into four source regions, China, ocean/local, Japan/Korea/Russia (J/K/R), and mixed (not falling into one of these three groups) (see Table SI1).

Further characterization of the ocean/local region was conducted by use of Cl^- concentrations in the aerosols as an oceanic indicator to further assess whether the ocean was a source or sink for SOCs in transit to HSO. None of the SOC concentrations was positively correlated with Cl^- . However, HCB, Dac, PCBs, Phe, Pyr, and Ret concentrations were negatively correlated with Cl^- concentrations. This may indicate that the ocean is a sink and not a source for SOCs in transit to HSO.

Meteorological and Source Region Variability. Figure 2 shows the temporal concentrations of the major SOCs measured during the campaign. To assess the impact of meteorological conditions on the SOC atmospheric concentrations at HSO, a multivariable linear regression model was developed by use of the SOC concentrations and site meteorological data (eq 2). Multivariable linear regression models have been previously used to assess the effect of meteorological conditions on SOC concentrations (14–16). In eq 2, WS (meters/second) represents the site wind speed, Sun [calories/(centimeter²-hour)] is the site sun intensity, WD (degrees) is the average site wind direction, ppt (millimeters/hour) is the precipitation summed for 4 days back in time for the back trajectory, JD is Julian days, and T (kelvins) is the average site temperature. Because the sample size was relatively small ($n = 18$) in comparison to the number of β terms ($n = 7$) in eq 2, a best subset method (Cp statistic) was used to find an equivalent model that only included statistically significant parameters (17). Results of the best meteorological subset model for each SOC are summarized in Table SI2, and the R^2 values ranged from 0.22 to 0.80.

$$\log(\text{concn}) = \beta_0 + \beta_1 JD + \beta_2 WS + \beta_3 Sun + \beta_4 \cos WD + \beta_5 \sin WD + \beta_6 ppt + \beta_7 1000/T \quad (2)$$

SOCs that existed primarily in the gas phase, operationally defined as SOCs measured in the PUF and XAD-2 fractions with <50% of their total concentration per sample measured on the quartz fiber filters (QFF), were generally influenced by wind speed, temperature, and/or Julian day. The gas-phase SOCs included all SOCs except for TPB, Lev, BaA, BbF, BkF, BeP, BaP, IcdP, DahA, and BghiP. In general, the concentration of gas-phase SOCs decreased with increasing wind speeds at HSO or Julian day and increased with

increasing temperature at HSO. α - and γ -HCH concentrations at HSO did not correlate significantly with meteorological variables.

Particulate-phase SOCs (TPB, Lev, BaA, BbF, BkF, BeP, BaP, IcdP, DahA, and BghiP), operationally defined as SOCs with >90% of their concentration measured on the QFF, were generally not influenced by meteorological variables. Of these particulate-phase SOCs, only TPB, BaP, and Lev showed correlations with meteorological parameters. TPB concentrations decreased with increasing wind speed at HSO. Concentrations of Lev, a marker for the combustion of biomass that originates from cellulose (18), decreased with increasing temperature at HSO, possibly due to decreased burning of biomass for heating as temperatures increased throughout the spring. For unknown reasons, BaP (a particulate-phase PAH) was the only SOC to show decreased concentrations with precipitation in transit to HSO.

After determination of the best meteorological subset model from eq 2, which took significant meteorological variables into account for each SOC, the differences in the source regions were investigated. This was conducted by adding the SRIF for each country to the best meteorological subset model. Equation 2 was not applied to DahA, Endo S, Hept, Met, DDTs, and Dield because of the low number of samples in which they were measured.

Combustion Byproduct Results. Figure 3 shows the proportion of variation (R^2) in the SOC concentrations that is explained by the best meteorological subset model and SRIF. Crosshatched bars indicate the proportion of variation in the SOC concentrations explained by best meteorological subset model only, and the unpatterned bars indicate the proportion of variation in the SOC concentrations explained when the SRIF is included in the model. Stars indicate the β term (slope) for the SRIF component of the model is negative, indicating decreasing SOC concentrations when the air mass came from the stated source region.

The particulate-phase PAHs (BbF, BkF, BeP, BaP, IcdP, and BghiP) showed increased concentrations when the source region was identified as China even after significant meteorological variables were taken into account (Figure 3). BaP was the only particulate-phase PAH to show significant correlation with meteorological parameters, while the other particulate-phase PAHs only included source region in the final model. ANT concentrations increased when ocean/local was identified as the source region, and concentrations decreased when the source region was identified as China. This is likely due to ANT's relatively short atmospheric lifetime relative to other gas-phase PAHs (19).

Xu et al. (20) recently estimated an emissions inventory of PAHs for China and pointed out the relatively high proportion of higher molecular weight (particulate-phase) PAHs emitted in China as compared to the Great Lakes Region of the United States. The major sources of these elevated concentrations of particulate-phase PAHs in China were attributed to domestic coal and firewood combustion, as well as the coking industry (20). Figure SI3 shows the PAH profile (normalized to phenanthrene) for the China PAH emission inventory estimated by Xu et al. (20), the PAH emission profile for the Great Lakes Region of the United States (21), and the average PAH profile we measured at HSO in samples where China, Japan/Korea/Russia, and ocean/local were identified as the major source region. The PAH profile from Xu et al. is for all of China, while the air masses we sampled at HSO originated from central and northern China. Xu et al. (20) point out that the provincial emission rates in China are "extremely different". Even with these regional differences, our results confirm that significant proportions of particulate-phase PAHs are being emitted from China.

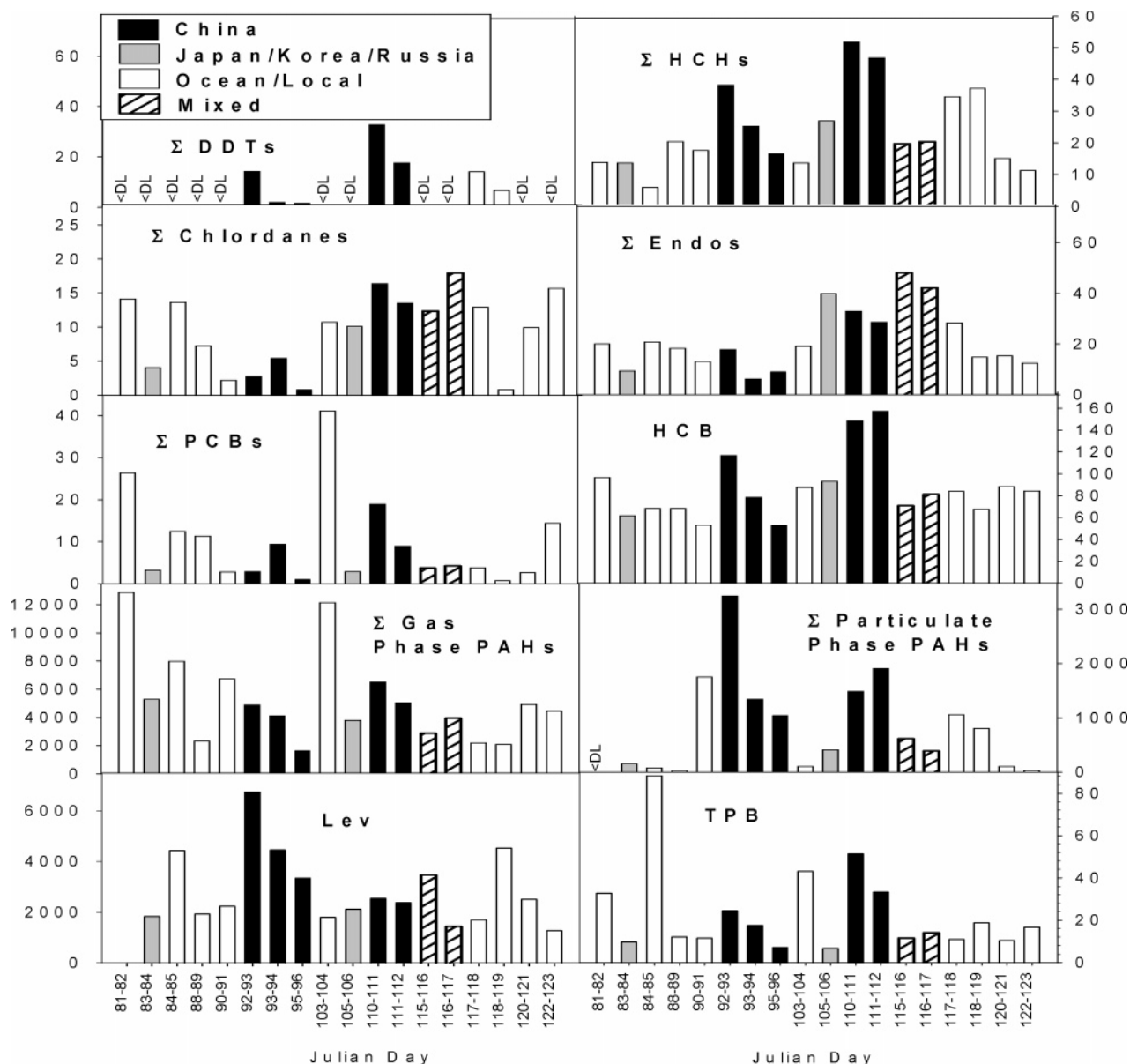


FIGURE 2. Temporal concentrations (picograms per cubic meter) of Σ chlordanes, HCB, Σ DDTs, Σ HCHs, Σ Endos, Σ PCBs, Σ particulate-phase PAHs, Σ gas-phase PAHs, TPB, and Lev. Patterns indicate source region. <DL indicates below the method detection limit. Lev could not be quantified in day 81–82 samples due to interference.

Because PAHs originate from combustion sources, a correlation with other combustion byproducts was investigated. Figure S14 shows the significant positive correlation (p value < 0.05) of Σ particulate-phase PAH concentration with submicrometer aerosol, black carbon (BC), Hg^0 , CO, SO_2 , and NO_x^* concentrations. Gas-phase PAHs did not show a significant correlation (p value > 0.05) with NO , Hg^0 , CO, SO_2 , or NO_x^* . A correlation between Hg^0 and CO concentrations has been previously reported for this sampling campaign and was attributed to coal combustion in China (10). The significant positive correlation between particulate-phase PAHs and Hg^0 , BC, and SO_2 concentrations suggests that coal combustion in China is a major source of particulate-phase PAHs.

FLA was the only gas-phase PAH that had a statistically significant correlation with the particulate-phase PAHs. Other researchers have noted enhancements in FLA concentrations as an indication of coal combustion (22, 23). Lev concentrations did not show a correlation with distinct source regions (Figure 3), although it did show a significant correlation (p

value 0.007) with the sum of particulate-phase PAH concentrations.

TPB has been measured in particles from solid waste incinerators and has recently been proposed as a marker for the combustion of plastics (24). There are 17 municipal solid waste incinerators (MSWIs) near HSO (16 on Okinawa and 1 on the neighboring island of Yoron). TPB concentrations were elevated at HSO in some ocean/local air masses (Figure 2) and showed a significant correlation (p value 0.015) with the gas-phase PAHs but not the particulate-phase PAHs. The TPB concentrations measured at HSO (0.007–0.088 ng/m^3) were lower than TPB concentrations measured in Sapporo, Japan (0.06–2 ng/m^3) (24).

PCB Results. PCBs were banned in Japan in 1972 (25), and production and use of PCBs has been banned or highly restricted since the early 1980s in China (26). However, PCB sediment fluxes have increased in the Pearl River Delta area of China (26). In an extensive passive air sampling campaign in the Asian region, elevated concentrations of PCBs were attributed to urban areas in both China and Japan (27).

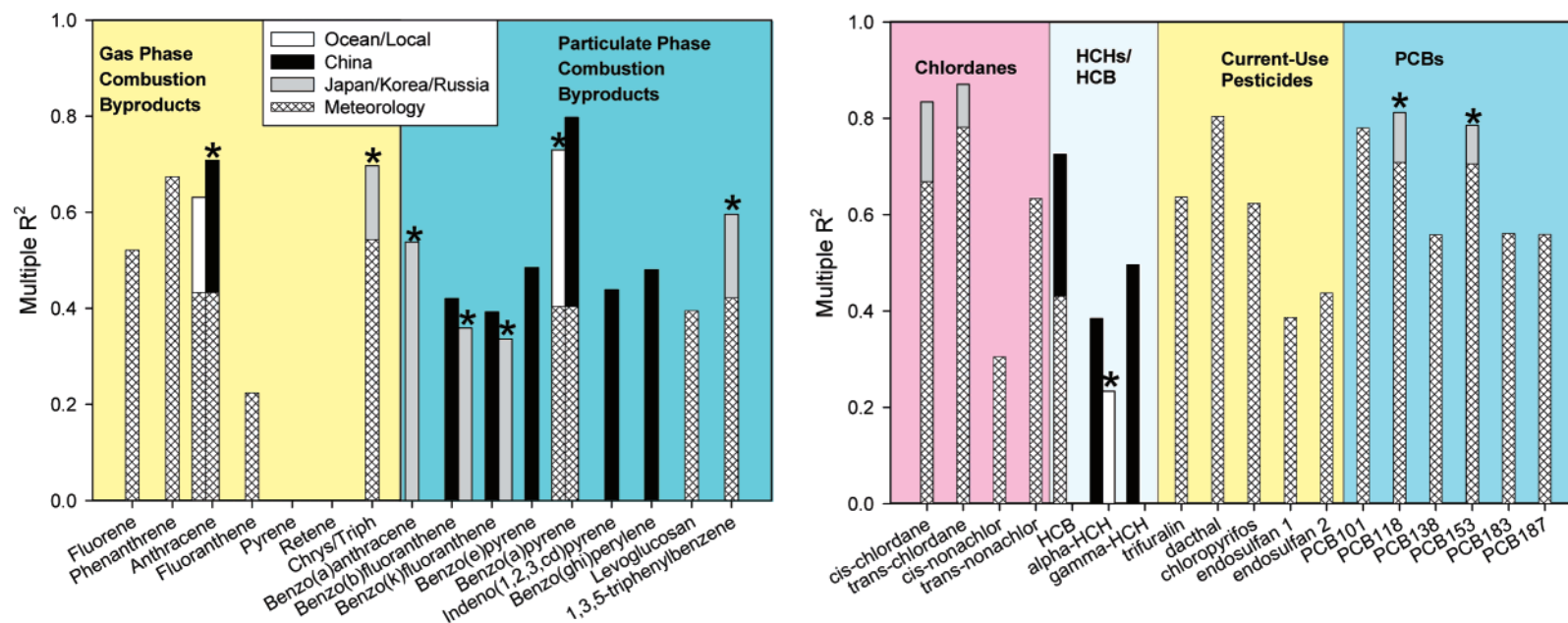


FIGURE 3. Results of multivariable linear regression model accounting for meteorological variables only (crosshatched bars) and SRIF (unpatterned bars). A star indicates the slope for the source term was negative, indicating decreasing SOC concentrations with increasing SRIF. Multiple bars indicate that, after accounting for meteorological variability, the SRIF was evaluated in the meteorological model separately due to multicollinearity between SRIFs.

Some of the highest concentrations of PCBs were measured in air masses from the ocean/Local region (Figure 2). PCBs 118 and 153 showed decreased concentrations when the source region was Japan/Korea/Russia (Figure 3). Additionally, the PCBs showed significant correlations with both gas-phase PAHs (p value < 0.0001) and TPB (p value 0.028). This correlation may indicate that PCBs, gas-phase PAHs, and TPB come from urban areas or that these SOCs are emitted from local sources, such as MSWIs (28).

Concentration ratios of the PCB congeners measured in this study were investigated to determine if there was a unique PCB ratio for different source regions (Figure SI5). The penta (PCB 101/PCB 118), hexa (PCB 153/PCB 138), and hepta (PCB 187/PCB 183) PCB ratios did not show any regional differences.

Pesticide Results. HCB, Σ HCHs, and Σ DDTs were all significantly correlated with one another (p value < 0.05) and showed elevated concentrations in air masses from China (Figures 2 and 3). HCB has many sources, including agricultural, industrial, and combustion sources (29). Previous research in Asia using passive air samplers showed elevated concentrations of HCB in China compared to other countries in the region (27). At HSO, HCB had the highest concentration of all of the organochlorine SOCs measured, with concentrations ranging from 53 to 157 pg/m^3 (Figure 2).

Both α - and γ -HCH showed elevated concentrations in air masses from China, and α -HCH concentrations decreased in ocean/local air masses (Figure 3). Technical HCH contains α - and γ -HCH and is banned in northeastern Asian countries (25). However, some stockpiles are believed to still exist (25). Lindane (γ -HCH) is still being produced and used in the region (25). In Korea, HCHs have been banned since 1979 (30). Although technical HCH was banned in China in 1983 (31), the facilities that produced technical HCH were not shut down until 2000 (32). Additionally, lindane has been used in China since 1991 (31). Technical HCH has primarily been used in southeastern China and lindane has primarily been used in northern China (31).

Because technical HCH is a mixture of several isomer of HCHs, the ratio of two of the isomers (α -HCH and γ -HCH) is commonly used to help identify the source. The technical mixture ratio (α : γ -HCH) ranges between 4 and 10 (25). Figure SI5 shows the α : γ -HCH ratio of the technical mixture, compared with the measured ratio at HSO. Only the China and Japan/Korea/Russia α : γ -HCH ratios were statistically different from each other (p value 0.04). The sample collected on Julian days 105–106 (Japan/Korea/Russia) was an outlier in the data set because it had an α : γ -HCH ratio of 6 and accounts for the statistical difference. The average α : γ -HCH ratio measured at HSO including all samples was 2.5 ± 1 . However, when the Julian days 105–106 sample was excluded, the ratio was 2.3 ± 0.5 .

DDT has been banned in Korea since 1973 (30) and was banned for all purposes in Japan in 1981 (25). In China, recent research has noted higher o,p' -DDT/ p,p' -DDT ratios than is expected from a technical mixture of DDT (33). This has been attributed to the use of Dicofol and its contamination with o,p' -DDT (33). China produces DDT for use in dicofol production and for export for use as a malaria control (33). The major use of dicofol is in south and central China, and applications typically occur in July and August (34). At HSO, p,p' -DDT was not detected; however, o,p' -DDT was measured primarily in samples associated with China (Figure 2). This may be due to dicofol use in China. Because the major usage of dicofol is in the summer, the o,p' -DDT concentrations measured at HSO in spring 2004 may be from revolatilization or fugitive emissions from production.

CC and TC concentrations increased in Japan/Korea/Russia air masses (Figure 3). Chlordane is banned in Russia and Korea (25). However, China and Japan still hold

exemptions for its use as a termiticide (25). Chlordane is used to kill termites in southern China (34) and is manufactured in eastern China (27). A recent passive air sampling campaign in the Asian region showed elevated concentrations of chlordanes in Japan as compared with other countries in the region (27).

TC is more susceptible to microbial degradation and photodegradation compared to CC (6, 35). Assuming the technical mixture TC/CC ratio in Asia is comparable to the technical mixture ratio in North America [which has been reported to be 1.26, 1.16, and 1.01 (6, 35, 36)], a ratio less than 1.0–1.26 would indicate a more aged source. At HSO, the TC/CC ratio averaged 1.2 ± 0.3 , which is similar to previously reported technical mixture ratios, with no distinct source region differences (Figure SI5). Additionally, the ratio of TC, CC, TN, and CN to the sum of chlordanes was similar to that for technical chlordane, with no distinct source region differences (Figure SI5). This indicates that fresh sources of chlordane dominate the atmospheric profile in this region.

Hept, a component of chlordane and a pesticide, is primarily banned in the region (25). In Korea, Hept was banned in 1979 (30). Hept concentrations at HSO were 4–60 pg/m^3 and it was measured in only six of the 18 samples collected. Hept concentrations were significantly correlated with Σ chlordane concentrations (p value 0.04). Heptachlor epoxide, a degradation product of Hept, was not detected in the HSO samples.

Technical endosulfan is 70% Endo I and 30% Endo II (15). In Korea, endosulfan has been used since 1971 and is applied in the summer (30). In China, endosulfan is also currently used (34). The likely source of endosulfans during the spring 2004 sampling campaign was revolatilization (temperature was a significant meteorological variable for Endo I) because the application time for endosulfan is summer. Endo I and II concentrations did not show any major source region differences (Figure 3). No differences existed in the Endo I/ Σ Endos and the Endo II/ Σ Endos ratios between the source regions (Figure SI5). The Endo I/ Σ Endos ratio averaged 0.92 ± 0.05 , and the Endo II/ Σ Endos ratio averaged 0.08 ± 0.04 . Both ratios differed from the technical mixture ratios of 0.70 and 0.30, respectively. The difference between the technical mixture and the measured ratios may be due to different formulations or it may be due to differences in their physical or chemical properties. The vapor pressures of Endo I and Endo II are 0.0061 and 0.0032 Pa (at 25 °C), respectively (37). If the major route of endosulfans to the atmosphere was revolatilization, a higher Endo I/ Σ Endos ratio would be expected.

Dield has not been used in China and is not currently in use in the countries in the northeastern Asian region (25). In Korea, dield was banned in 1971 (30). Dield was only detected in seven of the 18 samples at HSO and a source region could not be determined.

Trif, Chlorp, and Dac are all current-use pesticides that were measured at HSO. Meteorological variables explained a large proportion of the variation in Trif, Chlorp, and Dac concentrations (Figure 3). Met, an herbicide currently used on Okinawa, was detected in four of the 18 samples (Table SI1). Wind roses, calculated from site meteorological data, showed that on the days Met was measured, strong southeasterly winds passed directly over Okinawa prior to arriving at HSO. Met has a high water solubility and a relatively short estimated atmospheric lifetime (19), suggesting that on the days Met was measured at HSO, there was likely a contribution from local sources.

Emissions of SOCs from Asia. Jaffe et al. (10) used CO inventories for Asia and China and CO and Hg^0 measurements at HSO during this sampling campaign to calculate the emission of Hg^0 from Asia. They calculated that 1460 metric tons/year of Hg^0 are emitted from Asia (10). Three assump-

tions were made in the estimation of Hg^0 emission: (1) only dilution of CO and Hg^0 occurs in transit to HSO and there are no chemical or physical losses; (2) there is a constant source of both CO and Hg^0 ; and (3) the background concentrations of CO and Hg^0 are constant (10). Given the relatively short transit times to HSO from the source regions (24–48 h), these assumptions are reasonable.

We used this same approach to estimate the emission of FLA, BaA, CT, BbF, BkF, BeP, BaP, IcdP, and BghiP because these PAH concentrations were significantly correlated with CO concentrations (p value < 0.05). Because the majority of these PAHs were associated with particulate matter, we also calculated the emission of these same PAHs using BC measurements from HSO and a BC inventory (38). Although the PAH correlations with CO concentration were better than the correlations with BC concentration and the BC approach predicted higher PAH emissions, the emission estimates were within an order of magnitude of each other (Table S13). If the emission inventories for BC and CO are assumed to be equally accurate, then the emission calculations for the particulate-phase PAHs (BaA, BbF, BkF, BeP, BaP, IcdP, and BghiP) may be more accurately predicted by a particulate matter surrogate (BC). In contrast, for gas-phase PAHs such as FLA, the emission calculation based on CO would be more accurate.

The emissions of the seven carcinogenic PAHs (BaA, CHR, BbF, BkF, BaP, IcdP, and DahA) were estimated at 3460 tons in China in 2003 (20). United States emission estimates for these same seven PAHs were reported to be 2000 and 1400 tons in 1990 and 1996, respectively (20, 39). The calculated emission at HSO for six of the seven carcinogenic PAHs listed above (excluding DahA) was 1518–4179 metric tons/year for Asia and 778–1728 metric tons/year for China. DahA was only measured in five of the 18 samples and was not correlated with CO or BC. Our PAH emission estimates may be underestimated because the samples were collected in spring and do not reflect periods of high PAH emission (winter). Finally, *o,p'*-DDE, *p,p'*-DDE, *o,p'*-DDT, HCB, α -HCH, and γ -HCH concentrations were all significantly correlated (p value < 0.05) with CO concentrations, although this association was likely due to similar source regions and not similar sources.

Year-round measurements of SOCs at HSO are needed to better estimate SOC emissions and understand seasonal differences in East Asian outflow. These results confirm that East Asian outflow contains significant emissions of carcinogenic particulate-phase PAHs.

Acknowledgments

We thank Eric Prestbo and Frontier Geosciences (Seattle, WA), Takemitsu Arakaki of University of the Ryukyus, Okinawa, Shu Tao of Peking University, Will Hafner and Phil Swartzendruber of University of Washington—Bothell, and the Acid Deposition and Oxidant Research Center, Niigata, Japan for providing SO_2 , NO_x^* , and NO data. We thank the EPA: STAR Fellowship (to T.P.) and National Science Foundation CAREER (ATM-0239823) for funding. This work was made possible in part by the National Institutes of Health (Grant P30ES00210).

Supporting Information Available

Details of sample collection and site location; significant parameters and corresponding slope parameters used in the model; summary of meteorological parameters and SRIFs with the corresponding PCA plot used for source identification; figure comparing the HSO PAH profile to that of China and the Great Lakes; figure showing correlations between particulate phase PAHs and other incomplete combustion byproducts; and figure comparing SOC concentration ratios with technical mixture ratios. This material is available free of charge via the Internet at <http://pubs.acs.org>.

Literature Cited

- Wilkening, K. E.; Barrie, L. A.; Engle, M. Atmospheric science—Trans-Pacific air pollution. *Science* **2000**, *290*, 65–67.
- Killin, R. K.; Simonich, S. L.; Jaffe, D. A.; DeForest, C. L.; Wilson, G. R. Transpacific and regional atmospheric transport of anthropogenic semivolatile organic compounds to Cheeka Peak Observatory during the spring of 2002. *J. Geophys. Res., [Atmos.]* **2004**, *109*, D23S15.
- Harner, T.; Shoeib, M.; Kozma, M.; Gobas, F. A. P. C.; Li, S. M. Hexachlorocyclohexanes and endosulfans in urban, rural, and high altitude air samples in the Fraser Valley, British Columbia: Evidence for trans-Pacific transport. *Environ. Sci. Technol.* **2005**, *39*, 724–731.
- Jaffe, D.; Bertschi, I.; Jaegle, L.; Novelli, P.; Reid, J. S.; Tanimoto, H.; Vingarzan, R.; Westphal, D. L. Long-range transport of Siberian biomass burning emissions and impact on surface ozone in western North America. *Geophys. Res. Lett.* **2004**, *31*, L16106.
- Jaffe, D.; Anderson, T.; Covert, D.; Kotchenruther, R.; Trost, B.; Danielson, J.; Simpson, W.; Berntsen, T.; Karlsdottir, S.; Blake, D.; Harris, J.; Carmichael, G.; Uno, I. Transport of Asian air pollution to North America. *Geophys. Res. Lett.* **1999**, *26*, 711–714.
- Bailey, R.; Barrie, L. A.; Halsall, C. J.; Fellin, P.; Muir, D. C. G. Atmospheric organochlorine pesticides in the western Canadian Arctic: Evidence of transpacific transport. *J. Geophys. Res., [Atmos.]* **2000**, *105*, 11805–11811.
- Usenko, S.; Hageman, K. J.; Schmedding, D. W.; Wilson, G. R.; Simonich, S. L. Trace analysis of semivolatile organic compounds in large volume samples of snow, lake water, and groundwater. *Environ. Sci. Technol.* **2005**, *39*, 6006–6015.
- Kato, S.; Kajii, Y.; Itokazu, R.; Hirokawa, J.; Koda, S.; Kinjo, Y. Transport of atmospheric carbon monoxide, ozone, and hydrocarbons from Chinese coast to Okinawa island in the Western Pacific during winter. *Atmos. Environ.* **2004**, *38*, 2975–2981.
- Kanaya, Y.; Sadanaga, Y.; Nakamura, K.; Akimoto, H. Behavior of OH and HO_2 radicals during the Observations at a Remote Island of Okinawa (ORION99) field campaign 1. Observation using a laser-induced fluorescence instrument. *J. Geophys. Res., [Atmos.]* **2001**, *106*, 24197–24208.
- Jaffe, D.; Prestbo, E.; Swartzendruber, P.; Weiss-Penzias, P.; Kato, S.; Takami, A.; Hatakeyama, S.; Kajii, Y. Export of atmospheric mercury from Asia. *Atmos. Environ.* **2005**, *39*, 3029–3038.
- EPA. The analysis of polychlorinated dibenzo-*p*-dioxins and polychlorinated dibenzofurans by high-resolution gas chromatography/low resolution mass spectrometry (HRGC/LRMS). Method 8280A; U.S. Environmental Protection Agency: Washington, DC, 1996; <http://www.epa.gov/epaoswer/hazwaste/test/pdfs/8280a.pdf>.
- Draxler, R. R.; Rolph, G. D. HYSPLIT (Hybrid Single-Particle Lagrangian Integrated Trajectory) Model access via NOAA ARL READY Website (<http://www.arl.noaa.gov/ready/hysplit4.html>). NOAA Air Resources Laboratory: Silver Spring, MD, 2003.
- Wotawa, G.; Kroger, H.; Stohl, A. Transport of ozone towards the Alps—results from trajectory analyses and photochemical model studies. *Atmos. Environ.* **2000**, *34*, 1367–1377.
- Hafner, W. D.; Hites, R. A. Effects of wind and air trajectory directions on atmospheric concentrations of persistent organic pollutants near the great lakes. *Environ. Sci. Technol.* **2005**, *39*, 7817–7825.
- Burgoyne, T. W.; Hites, R. A. Effects of Temperature and Wind Direction on the Atmospheric Concentrations of α -Endosulfan. *Environ. Sci. Technol.* **1993**, *27*, 910–914.
- Goel, A.; McConnell, L. L.; Torrents, A.; Scudlark, J. R.; Simonich, S. Spray irrigation of treated municipal wastewater as a potential source of atmospheric PBDEs. *Environ. Sci. Technol.* **2006**, *40*, 2142–2148.
- Ramsey, F.; Schafer, D. W. *The Statistical Sleuth*; Duxbury: Pacific Grove, CA, 2002.
- Simoneit, B. R. T.; Elias, V. O.; Kobayashi, M.; Kawamura, K.; Rushdi, A. I.; Medeiros, P. M.; Rogge, W. F.; Dydik, B. M. Sugars-Dominant Water-Soluble Organic Compounds in Soils and Characterization as Tracers in Atmospheric Particulate Matter. *Environ. Sci. Technol.* **2004**, *38*, 5939–5949.
- EPI Suite; v3.12 ed.; U.S. Environmental Protection Agency: Washington, DC, 2000.
- Xu, S.; Liu, W.; Tao, S. Emission of Polycyclic Aromatic Hydrocarbons in China. *Environ. Sci. Technol.* **2006**, *40*, 702–708.
- Wu, C. Y.; Nelson, C.; Cabrera-Rivera, O.; Quan, J.; Asselmeier, D.; Baker, G.; McGeen, D. M.; McDonough, R.; Sliwinski, R.; Altenburg, R.; Velalis, T.; Judson, H.; Wong, P.; Wagemakers, J.;

- Moy, D. Analysis of Air Toxics Emission Inventories for Area Sources in the Great Lakes Region. U.S. Environmental Protection Agency: Washington, DC, 2001.
- (22) Simcik, M. F.; Eisenreich, S. J.; Lioy, P. J. Source apportionment and source/sink relationships of PAHs in the coastal atmosphere of Chicago and Lake Michigan. *Atmos. Environ.* **1999**, *33*, 5071–5079.
- (23) Larsen, R. K.; Baker, J. E. Source apportionment of polycyclic aromatic hydrocarbons in the urban atmosphere: A comparison of three methods. *Environ. Sci. Technol.* **2003**, *37*, 1873–1881.
- (24) Simoneit, B. R. T. M., P. M.; Didyk, B. M. Combustion Products of Plastics as Indicators for Refuse Burning in the Atmosphere. *Environ. Sci. Technol.* **2005**, *39*, 6961–6970.
- (25) United Nations Environment Programme. Regionally Based Assessment of Persistent Toxic Substances; Central and North East Asia. UNEP Chemicals: Châtelaine, GE, Switzerland, 2002.
- (26) Mai, B. X.; Zeng, E. Y.; Luo, X. J.; Yang, Q. S.; Zhang, G.; Li, X. D.; Sheng, G. Y.; Fu, J. M. Abundances, depositional fluxes, and homologue patterns of polychlorinated biphenyls in dated sediment cores from the Pearl River Delta, China. *Environ. Sci. Technol.* **2005**, *39*, 49–56.
- (27) Jaward, T. M.; Zhang, G.; Nam, J. J.; Sweetman, A. J.; Obbard, J. P.; Kobara, Y.; Jones, K. C. Passive air sampling of polychlorinated biphenyls, organochlorine compounds, and polybrominated diphenyl ethers across Asia. *Environ. Sci. Technol.* **2005**, *39*, 8638–8645.
- (28) Wikstrom, E.; Persson, A.; Marklund, S. Secondary formation of PCDDs, PCDFs, PCBs, PCBzs, PCPhs, and PAHs during MSW combustion. *Organohalogen Compd.* **1998**, *36*, 65–68.
- (29) Bailey, R. E. Global hexachlorobenzene emissions. *Chemosphere* **2001**, *43*, 167–182.
- (30) Yeo, H. G.; Choi, M.; Sunwoo, Y. Seasonal variations in atmospheric concentrations of organochlorine pesticides in urban and rural areas of Korea. *Atmos. Environ.* **2004**, *38*, 4779–4788.
- (31) Li, Y. F.; Cai, D. J.; Singh, A. Technical hexachlorocyclohexane use trends in China and their impact on the environment. *Arch. Environ. Contam. Toxicol.* **1998**, *35*, 688–697.
- (32) Tao, S.; Xu, F. L.; Wang, X. J.; Liu, W. X.; Gong, Z. M.; Fang, J. Y.; Zhu, L. Z.; Luo, Y. M. Organochlorine pesticides in agricultural soil and vegetables from Tianjin, China. *Environ. Sci. Technol.* **2005**, *39*, 2494–2499.
- (33) Qiu, X. H.; Zhu, T.; Yao, B.; Hu, J. X.; Hu, S. W. Contribution of dicofol to the current DDT pollution in China. *Environ. Sci. Technol.* **2005**, *39*, 4385–4390.
- (34) Qiu, X. H.; Zhu, T.; Jing, L.; Pan, H. S.; Li, Q. L.; Miao, G. F.; Gong, J. C. Organochlorine pesticides in the air around the Taihu Lake, China. *Environ. Sci. Technol.* **2004**, *38*, 1368–1374.
- (35) Hung, H.; Blanchard, P.; Halsall, C. J.; Bidleman, T. F.; Stern, G. A.; Fellin, P.; Muir, D. C. G.; Barrie, L. A.; Jantunen, L. M.; Helm, P. A.; Ma, J.; Konoplev, A. Temporal and spatial variabilities of atmospheric polychlorinated biphenyls (PCBs), organochlorine (OC) pesticides and polycyclic aromatic hydrocarbons (PAHs) in the Canadian Arctic: Results from a decade of monitoring. *Sci. Total Environ.* **2005**, *342*, 119–144.
- (36) Dearth, M. A.; Hites, R. A. Complete Analysis of Technical Chlordane Using Negative Ionization Mass Spectrometry. *Environ. Sci. Technol.* **1991**, *25*, 245–254.
- (37) Mackay, D.; Shiu, W. Y.; Ma, K. C. *Physical-Chemical Properties and Environmental Fate*; Chapman and Hall/CRCnetBase: Boca Raton, FL, 2000.
- (38) Streets, D. G.; Bond, T. C.; Carmichael, G. R.; Fernandes, S. D.; Fu, Q.; He, D.; Klimont, Z.; Nelson, S. M.; Tsai, N. Y.; Wang, M. Q.; Woo, J.-H.; Yarber, K. F. An inventory of gaseous and primary aerosol emissions in Asia in the year 2000. *J. Geophys. Res., [Atmos.]* **2003**, *108*, 8809.
- (39) Technology Transfer Network National Air Toxics Assessment. U.S. Environmental Protection Agency: Washington, DC, 2001.

Received for review September 21, 2006. Revised manuscript received March 7, 2007. Accepted March 8, 2007.

ES062256W